ELSEVIER

Chemical Engineering Journal 88 (2002) 233–243

Chemical Engineering Journal

www.elsevier.com/locate/cej

Pressure drop and flow regimes in cocurrent gas–liquid upflow through packed beds

T. Murugesan*, V. Sivakumar

Department of Chemical Engineering, Alagappa College of Technology, Anna University, Chennai 600 025, India

Received 27 September 2001; accepted 9 March 2002

Abstract

On the basis of the experimental results along with those available in the literature (1678 experimental data from five liquid systems, covering 10 different packings, from three sources) with a wide range of variables, a generalized approach is developed to identify the flow regime transitions viz., bubble flow, dispersed bubble flow and pulse flow in cocurrent two-phase (gas–liquid) upflow through packed beds. New correlations for the estimation of frictional pressure drop involving all the fundamental and operating variables are also presented for the three regimes of operation. This present correlations are more accurate than those previously reported.

Keywords: Packed bed reactors; Two-phase upflow; Pressure drop; Flow regimes

1. Introduction

Simultaneous contact of gas and liquid phases in a packed bed is commonly encountered in many of the chemical, biochemical, petroleum and petrochemical industries. The industrial application of these types of three phase contactors include Fischer–Tropsch synthesis, catalytic hydrosulfurization, hydrogenation and waste water treatment apart from its main application in biochemical reactions with supported enzymes or microorganism. The solids used for the packing may either be inert or catalyst, depending on the nature of operation. The mode of operation of three phase contactors are (i) countercurrent contact [1–7]; (ii) cocurrent downflow [8–10]; and (iii) cocurrent upflow [5,6,11–25] of both the phases. The hydrodynamic, heat and mass transfer conditions vary with the modes of operations [5,6]. The cocurrent upflow of both the phases is preferred for mass transfer operations due to better radial and axial distribution. As the liquid holdup is very high in cocurrent upflow reactors, the increase in interfacial area increases the mass transfer. Studies pertaining to the fluid mechanical aspects of the design and operation of two-phase cocurrent upflow through packed beds involving, overall pressure drop, identification of flow regimes, and phase holdup have been made both theoretically and experimentally by many investigators; some proposed correlations for the whole range of operations while others had developed predictive correlations using the identified flow regimes. The mixing and the dispersion characteristics of gas and liquid phases mainly depends upon the flow rates of the individual phases, physical properties, as well as the packing characteristics. Ford [11] and Eisenklam and Ford [12] are the first to observe different hydrodynamic regimes and later Turpin and Huntington, [13] Specchia et al. [14], Sato et al. [15], Saada [16], Fukushima and Kusaka [17], Mazzarino et al. [18], Goto and Gaspillo [19], Larachi et al. [20], Iliuta et al. [21] and Khan et al. [22] made significant contributions towards pressure drop and the delineation of flow regimes in two-phase (gas–liquid) upflow through packed beds. Apart from the review of Shah [5] on flow regimes and pressure drop, Larachi et al. [23] have made an extensive study on the two-phase pressure drop at high pressure conditions for a upflow packed bed and developed a correlation in terms of modified friction factor. Later, Molga and Westerterp [24] compared their data obtained using N_2-diethylamine and ethylene glycol systems and concluded that the correlation of Larachi et al. [23] is not satisfactorily representing their data. Even though much of work has been reported in literature for the estimation of two-phase pressure drop and identification of flow regimes, most of them are restricted to a limited range of applications, in terms of column geometry, physical properties of the phases and the characteristics of the packing materials etc. Since it is difficult to identify the boundaries of the flow regimes from first principles, the alternative approach

* Corresponding author. Tel.: +91-44-2351126.
E-mail addresses: tmgesan_57@yahoo.com, tmgesan@hotmail.com (T. Murugesan).

1385-8947/02/$ – see front matter
PII: S1385-8947(02)00039-6

Nomenclature

a_s	specific surface of particle (m^{-1})
d_c	column diameter (m)
d_e	hydraulic diameter $2d_p\phi\varepsilon/3(1-\varepsilon)$ (m)
d_h	Krischer and Kast hydraulic diameter $d_p(16\varepsilon^3/9\pi(1-\varepsilon)^2)^{1/3}$ (m)
d_p	particle diameter (m)
f_{LG}	friction factor $(\Delta P_f/z)d_h/2\rho_g U_g^2$
f_{TPf}	friction factor $(\Delta P_f/z)d_e/2\rho_g U_g^2$
Fr	Froude number $U^2/(gd_p)$
g	acceleration due to gravity ($m\,s^{-2}$)
G	gas mass velocity ($kg\,m^{-2}\,s^{-1}$)
h	$Re_g{}^{1.167}/Re_l{}^{0.767}$
L	liquid mass velocity ($kg\,m^{-2}\,s^{-1}$)
Mo	Morton's number $(g\mu_l^4/\rho_l\sigma_l^3)$
$(\Delta P)_f$	frictional pressure drop ($N\,m^{-2}$)
$(\Delta P)_T$	total pressure drop ($N\,m^{-2}$)
Re_g	gas Reynolds number $(d_p U_g\rho_g/\mu_g)$
Re_l	liquid Reynolds number $(d_p U_l\rho_l/\mu_l)$
U	velocity ($m\,s^{-1}$)
We_l	Weber number $(d_p U_l{}^2\rho_l/\sigma_l)$
X	parameter defined in Eq. (2)
X_{i-i}	inertial Lockhart–Martinelli dimensionless ratio $(U_g/U_l)(\rho_g/\rho_l)^{0.5}$
y	$(\Delta P/z)_{LG}/\{(\Delta P/z)_l + (\Delta P/z)_g\}$
Y	parameter defined in Eq. (3)
z	distance between pressure tapings (m)

Greek letters

χ	$(\Delta P/z)_l/(\Delta P/z)_g$
ε	voidage
ϕ	sphericity
λ	$X_{i-i}(Re_l * We_l)^{0.25}$
μ	viscosity ($kg\,m^{-1}\,s^{-1}$)
ρ	density ($kg\,m^{-3}$)
ρ_B	bulk density ($kg\,m^{-3}$)
ψ	$(\sigma_w/\sigma_l)[(\mu_l/\mu_w)(\rho_w/\rho_l)^2]^{0.33}$
σ	surface tension ($N\,m^{-1}$)

Subscripts

g	gas phase
l	liquid phase
w	water
LG	two-phase of liquid and gas

Superscripts

cal	calculated
exp	experimental

is to use empirical correlations based on the experimental observations. Hence, this present work is focused mainly on, to visually observe the flow regimes under different experimental conditions and to compare it with the pressure drop and to express the boundaries in terms of all variables affecting the hydrodynamics of the two-phase cocurrent upflow through packed beds and also to develop generalized correlations for the estimation of two-phase pressure drop for different regimes of operations identified in this study.

2. Experimental

All experiments were carried out in a perspex column (0.092 m i.d. and 1.2 m height). Fig. 1 gives the schematic diagram of the experimental column. The experimental column has the provision to feed the gas and liquid at the bottom of the column. The bottom of the packed section was provided with a gas distributor, whereas a gas–liquid separator was provided at the top. Liquid from the storage tank was pumped into the gas–liquid distributor using a centrifugal pump. Compressed air was fed into the bottom of the column through a pressure regulating valve. Rotometers with an accuracy of ± 2% were used for the measurement of individual phase flow rates. Facilities were provided for the simultaneous closure of both inlet and outlet valves. Provisions were also made for weighing the column for the estimation of phase hold up, using an electronic balance. Two pressure taps were provided for the pressure drop measurements. The detailed experimental procedure is given elsewhere [13,25]. In order to have a broader base for the analysis, literature data were also employed. The details of the data used for this present analysis are given in Table 1.

3. Results and discussions

Most of the developed correlations for the estimation of two-phase pressure drop are mainly based on the Lockhart–Martinelli [26] concept originally proposed for two-phase flow in horizontal pipes, which requires the in situ values of the single phase pressure drop. Otherwise, it is preferable to use Ergun's [27] type equation for the estimation of single phase pressure drop; but the empirical coefficients of the equation have to be determined using the experimental data. The present experimental data on pressure drop obtained for single phase system using water, with Raschig rings (dp = 0.0116 m) and spherical packings were compared with the available correlations of Larkins et al. [8] for its accuracy and the AARD are found to be 7.65% (bias = 0.99). A fair degree of agreement of the present experimental data with the values predicted using the published correlations confirms the validity of the present experimental results. From the measured total pressure drop, the frictional pressure drop was estimated using the following relation:

$$\frac{(\Delta P)_f}{z} = \frac{(\Delta P)_T}{z} - \rho_B g \quad (1)$$

where ρ_B is the bulk density of the gas–liquid mixture and z, the distance between the two pressure tapings. Fig. 2

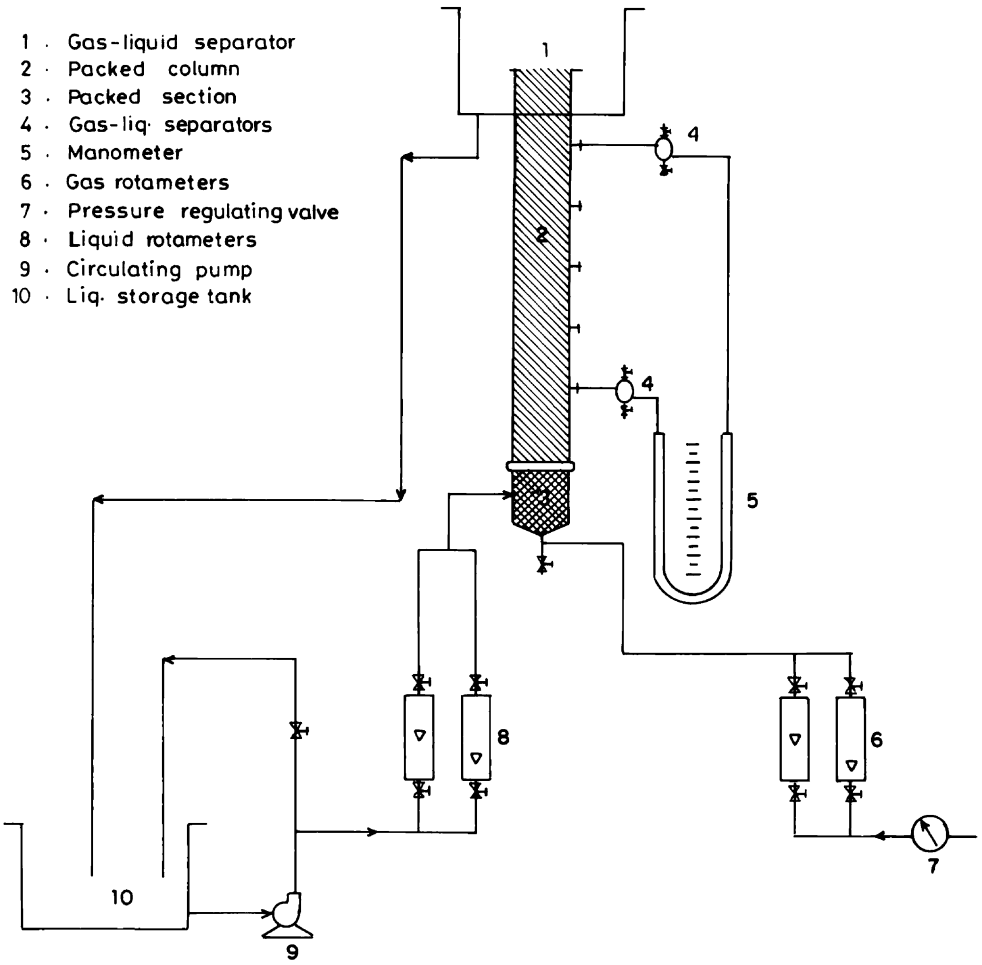

Fig. 1. Schematic diagram of the experimental setup.

shows the effect of gas and liquid flow rates on the frictional pressure drop. The frictional pressure drop increases with increasing phase flow rates as observed by Turpin and Huntington [13], Mazzarino et al. [18], Iliuta et al. [21], Srinivas and Chhabra [28], but the variation differs for three different conditions, i.e. (i) at both low gas and liquid flow rates, (ii) low gas flow rate with moderate increase in liquid flow rate (iii) at high liquid and gas flow rates, indicating the existence of three hydrodynamic flow regimes. The slopes and intercepts of the graphs were found to vary with the flow regimes and also vary with physical properties of the liquid systems, size and shape of the packing materials etc. By visual observation, the following flow patterns were observed, i.e. bubble flow, pulse flow and dispersed bubble flow. Since the interaction between the phases are different in three identified flow regimes, individual correlations for the prediction of pressure drop and the flow regime transition are advantageous. Based on the pressure drop measurements and the visual observations, the data are separated into three different groups representing three flow regimes for further analysis.

3.1. Flow regime identification

For low gas flow rates, gradual increase in liquid flow rates (i.e. the transition flow rate varies with physical properties and the size and shape of the packings) leads to the change in bubble flow regime (continous flow of liquid with dispersed bubbles) to dispersed bubble flow regime [29], where the presence of tiny as well as uniform size bubbles were noticed. Further increase in gas flow rate shifts both the bubble flow and dispersed bubble flow regime (depending on the liquid velocities) to the pulsed flow regime (high and low density pulses corresponding to high liquid and gas content, respectively moving rapidly upwards). Table 2 gives the details of the flow pattern boundaries proposed by various investigators. It is clear from the table that the identified flow boundaries are mainly based on the flow rates of the corresponding phases, except those of Saada [16] and Fukushima and Kusaka [17]. Of the available correlations, most of the authors prefer to use the plot of (L/G) versus G or sometimes G versus L, as the axis. It is also observed from the literature that most of the suggested co-ordinates

Table 1
Range of variable covered for the development of correlations

Variable			Range	
Mass flow rates				
Present work				
Liquid ($kg\,m^{-2}\,s^{-1}$)			4.5–135.4	
Gas ($kg\,m^{-2}\,s^{-1}$)			0.0065–0.391	
Khan [25]				
Liquid ($kg\,m^{-2}\,s^{-1}$)			1.239–44.435	
Gas ($kg\,m^{-2}\,s^{-1}$)			0.124–1.239	
PERC [30]				
Liquid ($kg\,m^{-2}\,s^{-1}$)			6.16–12.8	
Gas ($kg\,m^{-2}\,s^{-1}$)			1–6	
Bed characteristics		d_p (m)	ε	ϕ
Present work				
Particle 1	Raschig rings	0.004119	0.42	0.58
Particle 2	Raschig rings	0.01164	0.536	0.58
Particle 3	Berl saddles	0.01017	0.6345	0.3
Particle 4	Berl saddles	0.01375	0.7174	0.3
Particle 5	Spheres	0.0157	0.38	1
Khan [25]				
Particle 6	Raschig rings	0.006	0.48	0.58
Particle 7	Berl saddles	0.00857	0.62	0.3
Particle 8	Spheres	0.0062	0.39	1
PERC [30]				
Particle 9	Cylinders	0.003628	0.35	0.87
Particle 10	Cylinders	0.00727	0.35	0.87
Properties of fluids		Density ($kg\,m^{-3}$)	Viscosity ($kg\,m^{-1}\,s^{-1}$)	Surface tension ($N\,m^{-1}$)
Present work				
Water		1000	0.00085	0.072
Glycerol (25%)		1010	0.00172	0.069
Glycerol (56%)		1150	0.00405	0.069
Butyric acid (5%)		1000	0.001	0.0367
Khan [25]				
Water		1000	0.001	0.072
Mono-ethanol amine (MEA)		1020	0.015	0.0467
PERC [30]				
Water		1000	0.001	0.072

for the identification of flow boundaries, are mainly based on a limited number of data obtained using air–water systems and consequently do not allow the effect of all relevent variables. Unfortunately, no generalized quantitative criterion for identifying the flow regimes in a cocurrent packed bed upflow reactors is avaliable. Keeping this in view, in this present analysis it is proposed to identify the boundaries using the plot of $(U_l)^2$ versus $(U_g/U_l)^2$. Fig. 3 shows the boundaries of the identified flow regimes for three different conditions (i) air–water system using 0.004119 m diameter particle (shape factor = 0.58, bed voidage = 0.42). (ii) For the same particle, the regimes observed for air–56% glycerol system. (iii) For air–water system with particle of 0.0157 m diameter (shape factor = 1, bed voidage = 0.38). From the graphical analysis of the present data using the above mentioned coordinates, it is very clear that the flow pattern of phases moving cocurrently upwards through a packed bed is not only depend on the phase flow rates but also a function of particle size, shape, bed voidage and the fluid properties etc. Many times it is difficult to study the individual effect of particle shape and the bed voidage, since both are interlinked. In order to have a unified approach to generalize the boundaries of various flow regimes, this present observations along with flow boundaries reported in the literature [25,30] are employed. To have uniformity in the analysis, the dimensionless groups in the form of Fr, $(U^2/d_p g)$ of corresponding phases, (d_p/d_c) to represent the diameter ratio of particles to the column, ε, the bed porosity, and ϕ, the shape factor, are used. The optimized dimensionless property group in the form similar to the one suggested by Charpentier and Favier [31], i.e. $\psi = (\sigma_w/\sigma_l)[(\mu_l/\mu_w)(\rho_w/\rho_l)^2]^{0.33}$ is also used for correlating the data. Grouping the appropriate terms, it

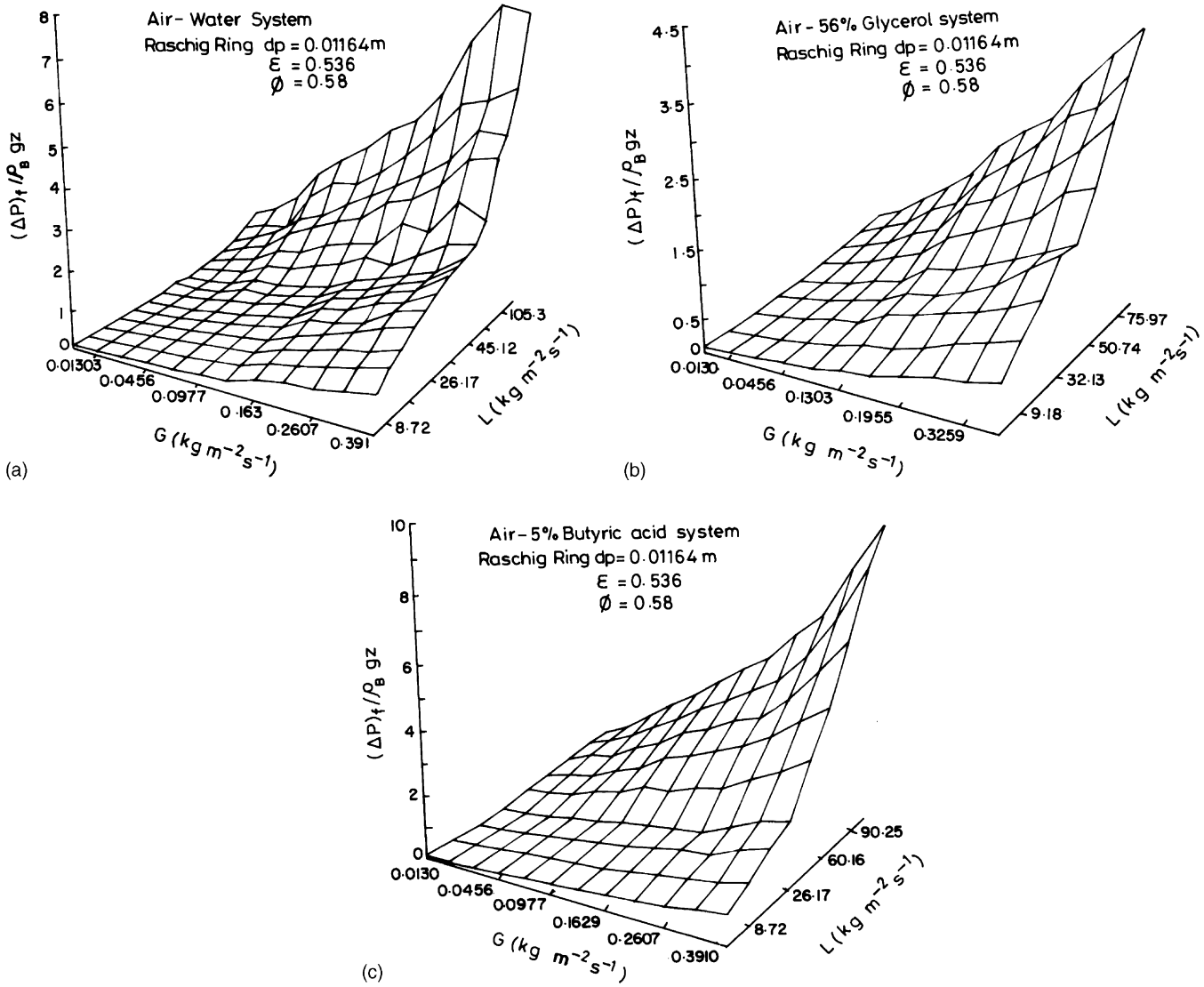

Fig. 2. (a) Effect of gas and liquid mass flow rates on $(\Delta P)_f/(\rho_B gz)$ for air–water system (a), for air–56% glycerol system (b), for air–5% butyric acid system (c).

is observed that the plot using the co-ordinates X versus Y, where

$$X = \left[Fr_l \left(\frac{d_p}{d_c} \right) \varepsilon^{-1.0} \right] \psi \tag{2}$$

$$Y = \frac{[(Fr_g/Fr_l)(\phi d_p/d_c)^{0.75}\varepsilon^{-1.0}]}{\psi} \tag{3}$$

in a log–log scale gives a better representation of all the available data (Table 1) on flow regime boundary transition and are shown in Fig. 4 which could be represented in the following form of relations:

3.2. Bubble flow regime

$$X \leq 1.75 \times 10^{-3}, \quad Y < 0.0112\, X^{-0.985} \tag{4}$$

3.3. Bubble to pulse regime

$$X \leq 1.75 \times 10^{-3}, \quad Y > 0.0112\, X^{-0.985} \tag{5}$$

3.4. Dispersed bubble regime

$$X \geq 1.75 \times 10^{-3}, \quad Y < 2.47 \times 10^{4} X^{1.32} \tag{6}$$

3.5. Dispersed bubble to pulse regime

$$X \geq 1.75 \times 10^{-3}, \quad Y > 2.47 \times 10^{4} X^{1.32} \tag{7}$$

It is interesting to note that the transition from bubble flow to dispersed bubble regime as observed by Iliuta et al. [21] (for air–water system, with $L = 17\,\mathrm{kg\,m^{-2}\,s^{-1}}$ and $G \leq 0.184\,\mathrm{kg\,m^{-2}\,s^{-1}}$) gives the valve of $X = 0.017$ which

Table 2
List of important literature flow map co-ordinates

Author	Co-ordinates	System	Variable range
Saada [16]	$[U_g^2 a_s/g\ \varepsilon^3](\rho_g/\rho_l)(\mu_l/\mu_w)^{0.2}$ versus $L/G(\rho_g/\rho_l)^{0.5}$	Air–water	$d_p = 0.000514$, 0.000974 and 0.002 (spheres) $G = 0.0147$–16.6 $L = 2$–205
Turpin and Huntington [13]	L/G versus G	Air–water	$d_p = 0.00762$ and 0.00823 (tubular alumina) $d_c = 0.05$, 0.1, 0.15 $G = 0.02$–6.5 $L = 6.5$–54
Speechia et al. [14]	L/G versus G	Air–NaOH	$d_p = 0.006$ (spheres, Berl saddles, Raschig rings) $G = 0.163$–2.57 $L = 2.5$–43 $\varepsilon = 0.4$–0.5
PERC [30]	L versus G	Air–water	$d_p = 0.003628$, 0.00727 (cylinder pellet) $G = 0.01$–15 $L = 1.23$–12.8
Sato et al. [15]	L versus G	Air–water	$d_p = 0.0026$, 0.0052, 0.008, 0.012 (spheres) $G = 0.06$–5 $L = 2.8$–140
Kukushima and Kusaka [17]	Re_g versus Re_l	Air–Na_2SO_4	$d_p = 0.0127$ and 0.02254 (ceramic beads) $G = 0.03$–2.5 $L = 1.5$–30
Mazzarino et al. [18]	L/G versus G	Air–water	$d_p = 0.003 \times 0.003$ (cylinder particle) 0.0017×0.004 (extrudates) $G = 0.08$–1.165 $L = 0.8$–6.3
Khan [25]	L versus G	Air–water Air–MEA	$d_p = 0.0062$, $\varepsilon = 0.39$, $\phi = 1$ (spheres) $d_p = 0.006$, $\varepsilon = 0.48$, $\phi = 0.58$ (Raschig rings) $d_p = 0.00857$, $\varepsilon = 0.62$, $\phi = 0.3$ (Berl saddles) $G = 0.075$–1.47 $L = 1.067$–46 $\mu_l = 0.001$–0.015

is in good agreement with this present proposed boundary between the bubble to dispersed bubble regime proving the validity of this generalized regime identification approach.

3.6. Two-phase pressure drop

The variation of two-phase frictional pressure drop with phase flow rates for the three different hydrodynamic regimes identified in this present study are shown in Fig. 5. Ford [11] and Saada [16] distinguished the flow regime into single phase and two-phase pore flow, and suggested separate pressure drop correlations for each regime and also gave the criterion for the transition from single phase pore flow to two-phase pore flow, whereas Turpin and Huntington [13] discriminated the flow into bubble flow, pulse flow and spray flow, however gave a single correlation for the estimation of pressure drop in terms of dimensionless parameters. The important literature correlations for two-phase pressure drop in cocurrent gas–liquid upflow through packed beds are given in Table 3. The applicability of the correlations due to Turpin and Huntington [13], Saada [16], Larachi et al. [23] and Khan [25] were tested using the present data (Table 1) along with those of Khan [25] and PERC [30]. The present experimental data obtained using air–water system (Raschig rings of diameter 0.004119 m) under bubble flow conditions alone compare favourably with the predicted values of pressure drop by the correlation of Larachi et al. [23] with an AARD of 12%, whereas the suggested correlation fails to represent all other data obtained using different systems and particles. The correlations of Saada [16], Turpin and Huntington [13] exhibit a tendency to overpredict the pressure drop for all the systems. Saada [16] and Turpin and Huntington [13] have used air–water system alone, for the development of correlations. Eventhough, Khan [25] has used air–water and air–MEA system, the effect of physical properties have not been properly accounted for their correlation. The estimated AARD are found to be very high in all the cases (Table 4), and the reason could be attributed to the fact that, the applicability of the avaliable correlations are restricted to a limited range of operation, interms of phase flow rates, particle dimensions and physical properties of liquids etc. The two-phase frictional pressure drop is due to the gas–liquid interfacial dissipation, along with liquid and gas packing dissipation. Friction between the fluids and the wall, and turbulence between the two-phases also cause the

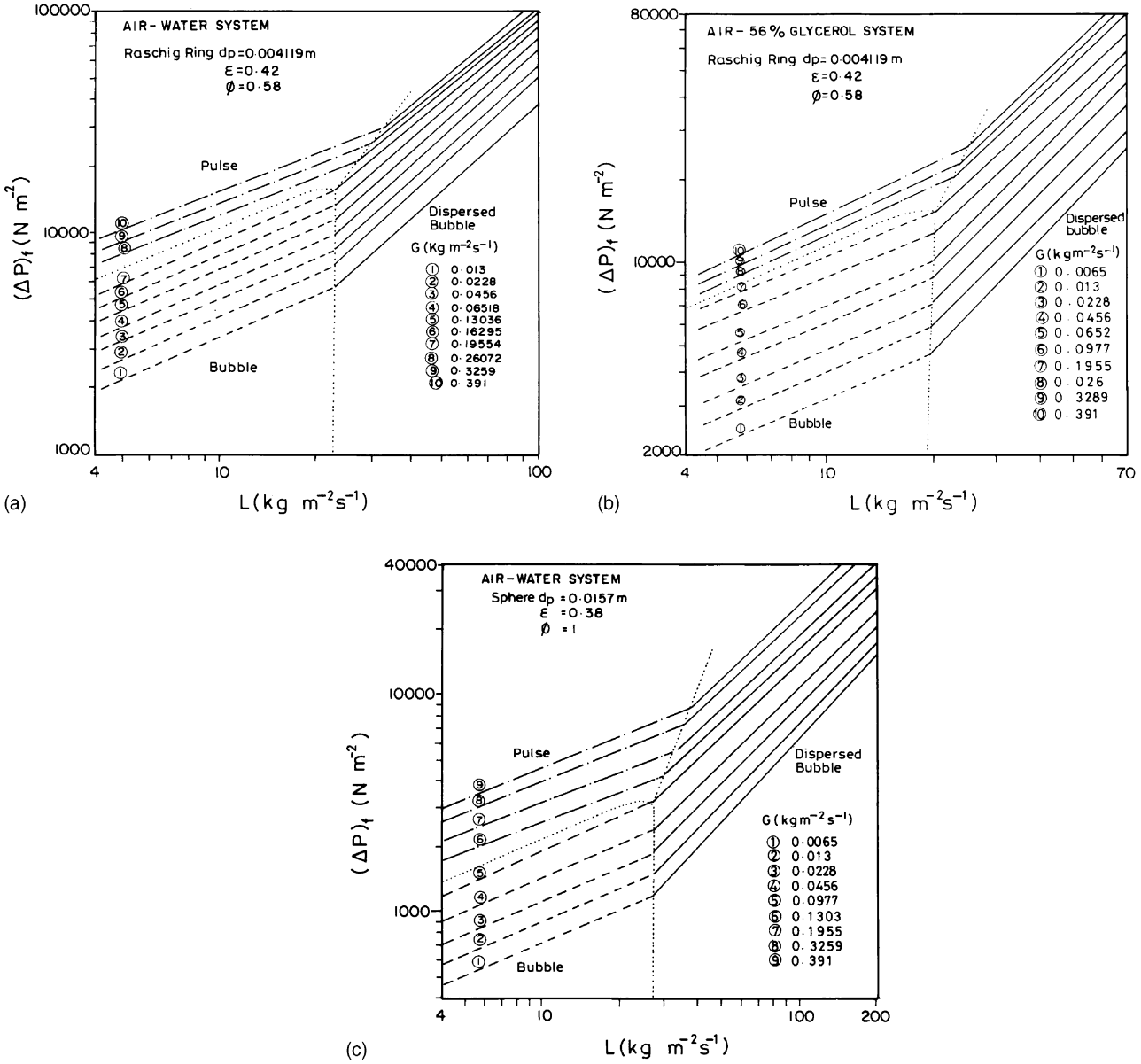

Fig. 3. Identification of flow regime boundary for air–water system with particle 1 (a), for air−56% glycerol system with particle 1 (b), for air–water system with particle 5 (c).

energy losses. Apart from the effect of liquid and gas flow rates, the effects of the particle size, shape, bed porosity and the fluid properties on two-phase pressure drop are also examined using the experimental results along with the published data. It is also observed from the present data that the frictional pressure drop is significantly higher for spheres as compared to berl saddles as packing. From the analysis of the data on pressure drop it is observed that the pressure drop decreases with the increase in bed voidage. The frictional pressure drop, during cocurrent gas–liquid upflow through packed beds, is mainly dependent on different hydrodynamic flow regimes of operation, which is a consequence of all fundamental variables as discussed earlier. From the graphical analysis of the available data, it is observed that the two-phase pressure drop is dependent on all the variables viz., phase flow rates, physical properties of the gas and liquid systems (density, viscosity and surface tension) and structural parameters of the porous medium (packing size and shape, bed porosity) used. Different combinations of the abovesaid variables were considered to formulate the dimensionless groups. Even though the liquid viscosity and the density have been accounted by using Reynold's Number, the combined effect of the liquid properties in the form of Morton's Number [20,31–35] have also been considered. The dimensionless two-phase frictional pressure drop, $(\Delta P)_f/\rho_B gz$, could be correlated in

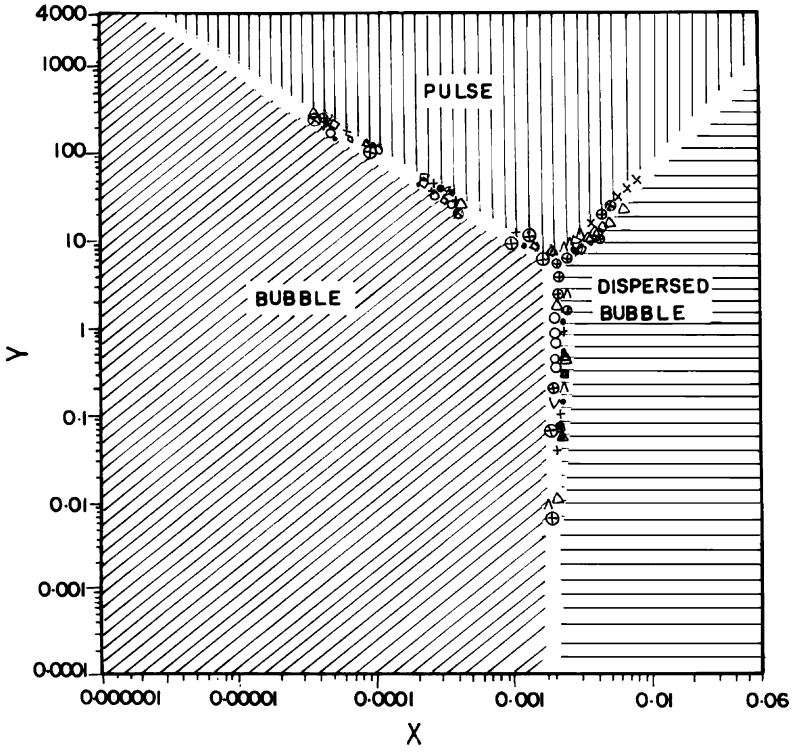

Symbol	Particle	System
+	Particle 1	Air – Water
•	Particle 2	Air – Water
⊕	Particle 3	Air - Water
⊡	Particle 4	Air - Water
■	Particle 5	Air - Water
o	Particle 1	Air-25% Glycerol
Δ	Particle 1	Air-56% Glycerol
∧	Particle 1	Air-5% Butyric acid
x	Particle 6	Air - Water
⊿	Particle 7	Air - Water
□	Particle 8	Air - Water
▽	Particle 7	Air - MEA
⊗	Particle 8	Air - MEA

Fig. 4. Flow regime discrimination based on present experimental and literature data.

the following form of general correlation:

$$\frac{(\Delta P)_f}{\rho_B g z} = C1\,(Re_l)^{a1}(Re_g)^{a2}\left(\frac{\varepsilon}{1-\varepsilon}\right)^{a3}\phi^{a4}\left(\frac{d_p}{d_c}\right)^{a5}(Mo)^{a6} \tag{8}$$

Regression analysis of data on bubble regime (377 data points), pulsed flow regime (212 data points) and dispersed bubble flow regime (748 data points) consisting of 1337 measurements obtained using four liquid systems with five different particles gave the constants and indices of the correlation for the three different regimes identified in the present work and the details are given below:

3.7. Bubble flow regime

$$\frac{(\Delta P)_f}{\rho_B g z} = 1.74\times 10^{-3}(Re_l)^{0.53}(Re_g)^{0.50} \times\left(\frac{\varepsilon}{1-\varepsilon}\right)^{-0.15}\phi^{0.32}\left(\frac{d_p}{d_c}\right)^{-2.1}(Mo)^{0.14} \tag{9}$$

3.8. Dispersed bubble flow regime

$$\frac{(\Delta P)_f}{\rho_B g z} = 2.5\times 10^{-4}(Re_l)^{1.11}(Re_g)^{0.47}\left(\frac{\varepsilon}{1-\varepsilon}\right)^{-0.17}\phi^{0.46} \times\left(\frac{d_p}{d_c}\right)^{-2.96}(Mo)^{0.26} \tag{10}$$

3.9. Pulse flow regime

$$\frac{(\Delta P)_f}{\rho_B g z} = 1.9\times 10^{-4}(Re_l)^{0.458}(Re_g)^{0.73} \times\left(\frac{\varepsilon}{1-\varepsilon}\right)^{-0.28}\phi^{0.452}\left(\frac{d_p}{d_c}\right)^{-2.2}(Mo)^{0.07} \tag{11}$$

In this present work, the average absolute value of the relative deviation (AARD) was adopted [20] to compare the predicted pressure drop values (using Eqs. (9)–(11)) with the experimental data.

$$\text{AARD} = \frac{1}{N}\sum_{i}^{N}\frac{\left|[\Delta p/z]_i^{exp} - [\Delta p/z]_i^{cal}\right|}{[\Delta p/z]_i^{exp}} \tag{12}$$

$$\text{Bias} = \exp\left(\frac{1}{N}\sum_{i}^{N}\ln\left(\frac{\Delta p/z_i^{exp}}{\Delta p/z_i^{cal}}\right)\right) \tag{13}$$

The statistical analysis (AARD and bias) of the applicability of the present as well as the available pressure drop correlation are made using 1678 experimental data (Table 1) and the results are given in Table 4, which clearly indicates that there is no need to complicate the developed expressions by considering individual data sets. The predictive ability of the correlations due to Saada [16], Turpin and Huntington [13], Larachi et al. [23] and Khan [25] along with this present proposed correlations (Eqs. (9) and (11)) are demonstrated in Fig. 6. The good agreement of the

Table 3
List of important literature correlations for pressure drop

Author	Correlation	System	Variable range
Ford [11]	Single phase pore flow $\Delta P/(z\rho_l g) = 0.024(Re_g)^{0.3}\ (Re_l)^{0.67}\ (\mu_l/\mu_g)^{0.8}$ Two-phase pore flow $\Delta P/(z\rho_l g) = 0.0407(Re_g)^{0.57}\ (Re_l)^{0.29}\ (\mu_l/\mu_g)^{0.28}$	Air–water	$d_p = 0.001$ $d_c = 0.01$
Saada [16]	Single phase pore flow $\Delta P/(z\rho_l g) = 0.024(Re_g)^{0.39}\ (Re_l)^{0.6}\ (d_p/d_c)^{-1.1}$ Two-phase pore flow $\Delta P/(z\rho_l g) = 0.027(Re_g)^{0.51}\ (Re_l)^{0.35}\ (d_p/d_c)^{-1.15}$	Air–water	$d_p = 0.000514$,0.000974 and 0.002 (spheres) $G = 0.147$–16.6 $L = 2$–205
Turpin and Huntington [13]	$\ln f_{TPf} = 8 - 1.12(\ln h) - 0.0769(\ln h)^2 + 0.0152(\ln h)^3$ $(0.3 \geq h \geq 500)$	Air–water	$d_p = 0.00762$ and 0.00823 (tubular alumina) $d_c = 0.05$, 0.1, 0.15 $G = 0.02$–6.5 $L = 6.5$–54
Larachi et al. [23]	$f_{LG} = \lambda^{-1.5}(45.6 + (15.9\lambda^{-0.5}))$, where $\lambda = X_{i-i}$ $(Re_l We_l)^{0.25}\ X_{i-i} = (U_g/U_l)\ (\rho_g/\rho_l)^{0.5}$	Helium–water Nitrogen–water Argon–water CO_2–water N_2–ethylene glycol	$d_p = 01.0033$ (polyethylene cylinder loaded with talc) $G = 0$–1.7 $L = 6.6$–13.2 $P = 0.3$–5.1 $\varepsilon = 0.38$
Goto and Gaspillo [19]	$\log y = 0.55$ /[{(log(χ/1.2)}^{2} + 0.666] $y = (\Delta P/z)_{LG}/\{(\Delta P/z)_l + (\Delta P/z)_g\}$ $\chi = (\Delta P/z)_l/(\Delta P/z)_g$	Air–0, 11.5 and 20% propylene glycol in water	$d_p = 0.00045$, 0.00092 and 0.000183 (glass beads) $G = 0.05$–2 $L = 1$ $\rho_l = 998$–1016 $\mu_l = 0.0001$–0.002
Khan [25]	Bubble regime $(\Delta P/z)_f = 1800\ L^{0.93}\ G^{0.6}\ (1-\varepsilon)^{1.5}/\varepsilon$ Pulse regime $(\Delta P/z)_f = 4500\ L^{0.62}\ G^{0.75}\ (1-\varepsilon)^{1.5}/\varepsilon$ Spray regime $(\Delta P/z)_f = 10000\ L^{0.2}\ G^{1.25}\ (1-\varepsilon)^{1.5}/\varepsilon$	Air–water Air–MEA	$d_p = 0.0062$, $\varepsilon = 0.39$, $\phi = 1$ (spheres) $d_p = 0.006$, $\varepsilon = 0.48$, $\phi = 0.58$ (Raschig rings) $d_p = 0.00857$, $\varepsilon = 0.62$, $\phi = 0.3$ (Berl saddles) $G = 0.075$–1.47 $L = 1.067$–46 $\mu_l = 0.001$–0.015

Table 4
Statistical comparison of pressure drop correlations with present and literature data

Correlation		Present data		Khan data [25]		PERC data [30]	
		AARD (%)	Bias	AARD (%)	Bias	AARD (%)	Bias
Saada [16]	Single phase pore flow	5576	0.138	4839	0.15	–	–
	Two-phase pore flow	3107	0.035	1690	0.09	1221	0.085
Turpin and Huntington [13]	–	66.13	1.3	110	0.76	107.7	0.92
Larachi et al. [23]	–	68	3.64	55.8	2.3	66.6	3.5
Khan [25]	Bubble regime	46	1.347	16.62	1.1	–	–
	Pulse regime	29	1.214	15.4	1.1	71.5	1.2
Present correlation	Eq. (9)	9.52	1.07	8.1	1.05	–	–
	Eq. (10)	7.9	0.99	11.2	0.98	–	–
	Eq. (11)	7.1	1	13.1	0.985	12.7	1.15

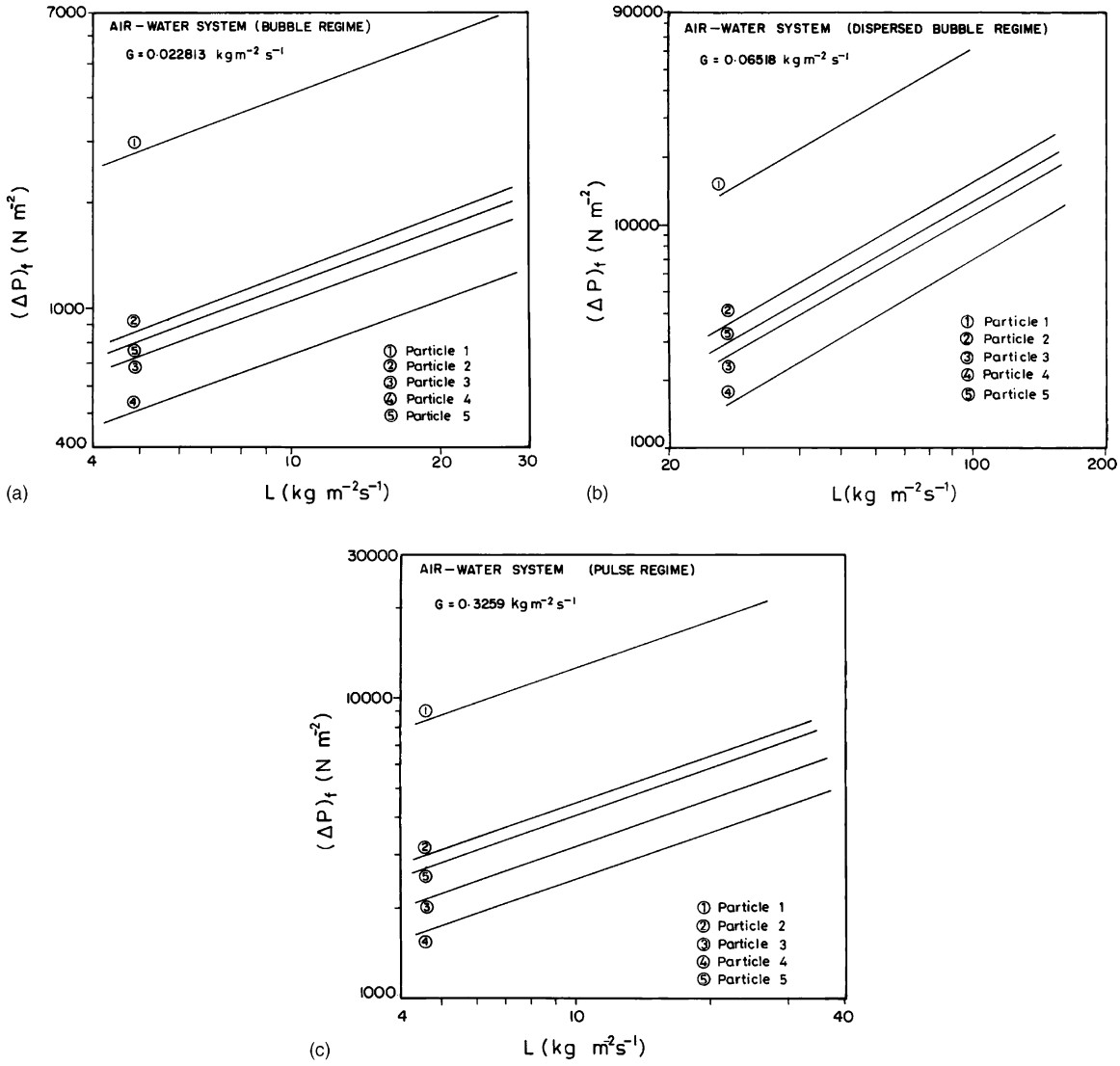

Fig. 5. Effect of phase flow rates on frictional pressure drop for bubble regime (a), for dispersed bubble regime (b), for pulse regime (c).

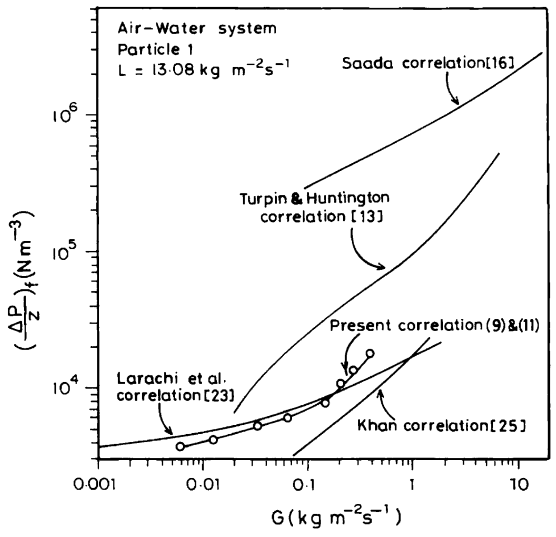

Fig. 6. Comparison of experimental data with literature correlation.

results (Table 4 and Fig. 6) proves that the present proposed correlations (Eqs. (9)–(11)) outperforms the other available literature correlations, as it covers wider range of variables (Table 1).

4. Conclusion

On the basis of the present investigation, using 1678 experimental data (five liquid systems and 10 different particles), it is confirmed that the hydrodynamics of two-phase upflow through packed beds, i.e. the flow regime transitions and the frictional pressure drop are strongly influenced by all the fundamental as well as the operating variables of the systems considered. A unified empirical approach was established for the estimation of flow regime transitions for all the available data. Empirical correlations for pressure drop were made for three identified flow regimes. A good agreement between the estimated pressure drop using the present

developed correlations (Eqs. (9)–(11)) and the measured pressure drop was demonstrated.

Acknowledgements

The authors wish to express their appreciation to UGC for financial assistance for the fabrication of experimental set up and to CSIR for the award of senior research fellowship to V. Sivakumar for the support of this investigation.

References

[1] J.C. Charpentier, Chem. Eng. J. 11 (1976) 161.
[2] J.S. Eckert, Chem. Eng. Prog. 57 (1961) 54.
[3] I.A. Furzer, R.W. Michell, AIChE J. 16 (1970) 380.
[4] F. Morton, P.J. King, B. Alkinson, Trans. Inst. Chem. Eng. 42 (1970) 380.
[5] Y.T. Shah, Gas–liquid–solid Reactor Design, McGraw-Hill, New York, 1979.
[6] T.B. Zhukova, V.N. Pisarenko, V.V. Kofarov, Int. Chem. Eng. 30 (1990) 57.
[7] I. Iliuta, F.C. Thyrion, L. Bole, M. Giot, Chem. Eng. Tech. 20 (1997) 171.
[8] R.P. Larkins, R.R. White, D.W. Jeffrey, AIChE J. 7 (1961) 231.
[9] Y. Sato, T. Hirose, F. Takohashi, M. Toda, J. Chem. Eng. Jpn. 6 (1973) 147.
[10] P.S.T. Sai, Y.B.G. Varma, AIChE J. 33 (1987) 2027.
[11] L.H. Ford, Flow through porous media with special reference to turbulent regime, Ph.D. Thesis, University of London, London, 1960.
[12] P. Eisenklam, L.H. Ford, Inst. Chem. Engrs London, June 1962, p. 333.
[13] J.L. Turpin, R.L. Huntington, AIChE J. 13 (1967) 1196.
[14] V. Specchia, S. Sicardi, A. Gianetto, AIChE J. 20 (1974) 646.
[15] Y. Sato, T. Hirose, T. Ida, Kagaku Kogaku 38 (1974) 543.
[16] M.Y. Saada, Chem. Eng. 19 (1975) 371.
[17] S. Fukushima, K. Kusaka, J. Chem. Eng. Jpn. 12 (1979) 296.
[18] I. Mazzarino, S. Sicardi, G. Baladi, Chem. Eng. J. 36 (1987) 151.
[19] G. Goto, P.D. Gaspillo, Ind. Eng. Chem. Res. 31 (1992) 629.
[20] F. Larachi, Z. Bensetiti, B.P.A. Grandjean, G. Wild, Chem. Eng. Tech. 21 (1998) 11.
[21] I. Iliuta, F.C. Thyrion, O. Muntean, Chem. Eng. Sci. 51 (1996) 4987.
[22] A. Khan, A.A. Khan, Y.B.G. Varma, Bioprocess Eng. 16 (1997) 355.
[23] F. Larachi, G. Wild, A. Laurent, N. Midoux, Ind. Eng. Chem. Res. 33 (1994) 519.
[24] E.J. Molga, K.R. Westerterp, Ind. Eng. Chem. Res. 36 (1997) 622.
[25] A. Khan, Flow pattern of the phases phase holdup and pressure drop in concurrent gas–liquid upflow through packed beds, Ph.D. Thesis, IIT, Chennai, 1998.
[26] R.W. Lockhart, R.C. Martinelli, Chem. Eng. Prog. 45 (1949) 39.
[27] S. Ergun, Chem. Eng. Prog. 48 (1952) 89.
[28] K.V. Srinivas, R.P. Chhabra, Can. J. Chem. Eng. 72 (1994) 1085.
[29] I. Iliuta, F.C. Thyrion, L. Bolle, M. Giot, Chem. Eng. Tech. 20 (1997) 171.
[30] D. Smith, A. Reznik, A. Pontello, Pitsburg Energy Research Center Quarterly Reports, (1975–1976), Personal Communication.
[31] J.C. Charpentier, M. Favier, AIChE J. 21 (1975) 1213.
[32] L.S. Fan, F. Bavarian, R.L. Gorowara, B.E. Kreischer, Powder Tech. 53 (1987) 285.
[33] D. Skala, V. Veukovic, Can. J. Chem. Eng. 66 (1988) 192.
[34] G.H. Song, F. Bavarian, L.S. Fan, Can. J. Chem. Eng. 67 (1989) 262.
[35] P. Kalaichelvi, T. Murugesan, J. Chem. Tech. Biotech. 69 (1997) 130.